JOURNAL OF CATALYSIS **124**, 22–29 (1990)

CO Chemisorption on the [111] and [100] Oriented Single Crystal Surfaces of the Alloy $CoPt_3$[1]

U. BARDI,* B. C. BEARD,†,[2] AND P. N. ROSS†

**Dipartimento di Chimica, Universita di Firenze, 50121 Firenze, Italia; and †Materials and Chemical Sciences Division, Lawrence Berkeley Laboratory, 1 Cyclotron Road, Berkeley, California 94720*

Received July 26, 1989; revised December 4, 1989

In a previous study, it was shown that surfaces of both the [111] and [100] oriented single crystals of $CoPt_3$ have a "sandwich" structure having an outermost atomic layer that is essentially pure Pt and a second layer enriched in Co (with respect to the bulk). In the present work, we report a study of the energetics of carbon monoxide chemisorption on these surfaces and compare the results with our previous study of carbon monoxide adsorption on Pt_3Ti surfaces. A surprising similarity in the activation energy for desorption of carbon monoxide from Pt sites on both the $CoPt_3$ and the Pt_3Ti surfaces was found, with the adsorption energy being substantially lower on the alloy surfaces than on the pure Pt surfaces of the same orientation. Since the $CoPt_3$ surfaces have a pure Pt top layer, it appears that the intermetallic bonding between Co in the second layer and Pt in the top layer changes the electronic states available for the bonding of carbon monoxide to the surface.

1. INTRODUCTION

Alloy surfaces have been the object of numerous surface science studies investigating the structural and adsorptive properties in order to develop a better understanding of catalysis by alloys. Binary alloys composed of platinum and one electropositive metal are of interest from a fundamental point of view, since they often form intermetallic compounds with highly negative enthalpies of formation (*1*) and with ordered structures at characteristic bulk compositions, and may have ordered surface structures with unique catalytic properties. When both metals are present in the surface, the catalytic and adsorptive properties may be affected both by the formation of intermetallic bonds (*2, 3*) and by the dispersion on the solute metal in the surface (*4, 5*).

Of particular interest to us is the trend in surface chemistry for the binary alloys of nominal composition Pt_3M when M changes across the $3d$ transition metals, e.g., $M = Ti(d^3s)$ to $Cu(d^{10}s)$. The trend in the bulk structure of these alloys indicates that as the $3d$ occupation increases, i.e., as the M metal becomes more electronegative, the heat of formation of the alloy decreases (*1, 9*), the order–disorder transition temperature decreases (*10*), and the composition range for the formation of ordered phases narrows (*9, 10*). We have reported previously (*6–8*) detailed studies of the surface chemistry of the alloy Pt_3Ti,[3] which has a very negative enthalpy of formation (−20.7 kcal/g at.) and has an ordered bulk phase with the $L1_2$ structure with a critical temperature above 1500°K. These studies have shown that Pt_3Ti forms clean annealed low index surfaces that are ordered and are simple truncations of the bulk $L1_2$ structure.

---

[1] The U.S. Government's right to retain a nonexclusive royalty-free license in and to the copyright covering this paper, for governmental purposes, is acknowledged.

[2] Present address: White Oak Laboratory, Naval Surface Weapons Center, Silver Springs, MD.

[3] The IUPAC convention for intermetallic compounds is to place the elements in alphabetical order. Hence, we use here $CoPt_3$ and Pt_3Ti as the symbols for the 75% Pt binary alloys.

0021-9517/90 $3.00

However, Paul *et al.* (*11*) reported a different surface composition for $Pt_3Ti(111)$, although they also saw the same $p(2 \times 2)$ LEED pattern that is expected for the surface formed by bulk truncation (*8*). On the basis of LEISS Ti/Pt ratios and variable take-off angle XPS intensity ratios, they concluded that the surface of $Pt_3Ti(111)$ was pure Pt, with a Ti-rich second layer. They did not explain how such a structure could produce a $p(2 \times 2)$ LEED pattern. Also, Paul *et al.* did not find any evidence for dissociation of CO on their $Pt_3Ti(111)$ surface, consistent with the properties of CO on a pure Pt surface, whereas Bardi *et al.* found that a fraction of the CO adsorbed at 220 K dissociated upon rapid heating of the sample to 1000 K, consistent with the properties of a surface containing Ti in the outermost layer. It is possible that the exact procedures for cleaning and annealing the Pt_3Ti crystal played a critical role in determining whether or not Ti is present in the top layer. Nonetheless, both studies produced *identical* thermal desorption spectra for the CO desorbing molecularly from the $Pt_3Ti(111)$ surface and attributed the differences in TDS compared to pure Pt(111) to the effects of intermetallic bonding.

In the present work, we report a study of the surface chemistry of the alloy $CoPt_3$ and compare the chemistry of CO adsorption to that observed on Pt_3Ti. Cobalt is not as electropositive a metal as Ti, the heat of formation of the $CoPt_3$ alloy is much lower (−3 kcal/g atom versus −20) and the alloy as we used it was *not ordered* in the bulk. Using a combination of LEED and low-energy ion-scattering spectroscopy (LEISS), we found (*12*) that the clean annealed alloy surfaces of both the [111] and [100] orientations are essentially pure Pt, e.g., less than 2 at.% Co. We found that the chemistry of carbon monoxide adsorption on $CoPt_3$ appeared to have some similarities to that on Pt_3Ti and to be energetically quite different from that on either pure metal surface.

2. EXPERIMENTAL

The Co–Pt alloy was prepared by arc melting the pure elements in inert atmosphere in the proportion of 3Co : 1Pt. Single crystal samples were obtained by repeated zone refining under vacuum. Elemental analysis of the single crystal samples by X-ray fluorescence indicated some loss of Co occurred during the zone refining. Thus, the notation of $CoPt_3$ for this alloy is primarily for convenience, the alloy being slightly substoichiometric. X-ray examination of the single crystal samples before surface studies were performed showed that the bulk alloy was ordered, with the *fcc* $AuCu_3$ type ($L1_2$) structure and a lattice constant of 3.85 Å, corresponding to a 1.8% contraction with respect to pure platinum (a = 3.924 Å). This value is in agreement with the value reported (*10a*) for the lattice parameter of stoichiometric $CoPt_3$ (3.831 Å). However, X-ray diffraction analyses performed *after* the samples underwent thermal treatments during the UHV study showed that the alloy was disordered (disordered meaning a random substitution of Co for Pt in the *fcc* lattice versus an ordered substitution of Co for Pt at the corners of the unit cell), but the interatomic distance was not significantly changed. The critical temperature for the order–disorder transition in $CoPt_3$ is a relatively low 850°K (*10b*), lower than the annealing temperature we used to obtain clean surfaces with sharp LEED patterns, e.g., 1000°K. Apparently, the high-temperature disordered structure was quenched when the crystals cooled from the annealing conditions typically used in our UHV chamber.

Disk-shaped single crystal samples oriented along the [111] and [100] axes were cut from the single crystal rod and mechanically polished. The disks were gold brazed to tantalum foil. The foil was held to a sample manipulator by spotwelded tantalum wires which were also used to anneal the sample by resistive heating. A chromel–alumel thermocouple was spotwelded to the tantalum foil for temperature measurements. Cleaning of the sample surface could usually be obtained by means of cycles of Ar ion bombardment and annealing in UHV at or over 900°K. This treatment was not always sufficient for the complete removal of the carbon surface contamination, which could be obtained by annealing the ion-bombarded surface in the presence of a low (ca. 1×10^{-8} Torr) pressure of oxygen.

Surface analyses by LEED, AES, ARXPS, and LEISS were performed as described previously (*12*). Carbon monoxide desorption spectroscopy was done by dosing the clean annealed surfaces with CO (Matheson research grade) at room temperature and at a pressure of 1×10^{-7} Torr for 10–10^3 s (1–100 Langmuirs), then heating the crystals at a rate of 14°/s (the [100] sample) or 16°/s (the [111] sample). The quantity of CO desorbed as a function of time/temperature was determined with a quadrupole mass spectrometer (Leybold–Hereus Model IQ-200).

3. RESULTS AND DISCUSSION

3.1 LEED

The LEED pattern exhibited by the clean, annealed [111] oriented surface had simple hexagonal symmetry with no "superlattice" reflections due to ordered cobalt substitution in the surface, in contrast to the superlattice pattern we observed for $Pt_3Ti(111)$ (*8*).

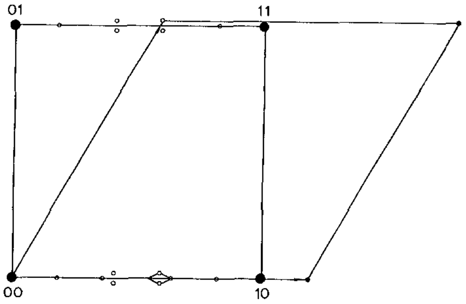

FIG. 1. Schematic of LEED pattern for the clean annealed surface of $CoPt_3(100)$.

A schematic for the LEED pattern for the clean, annealed [100] oriented surface is shown in Fig. 1. The spots at the vertices of the "square" in this pattern are those of a unit cell which has essentially the same structural parameters as those of an unreconstructed Pt(100) surface. The rows of "extra spots" which appear along the sides of the unit cell are due to a surface reconstruction. A detailed discussion of the analysis of this LEED pattern is given elsewhere (*12b*). The best description of the pattern, in terms of a coincident lattice, is a $c(58 \times 22)$ mesh. LEISS analysis indicated that the composition of the surface associated with the $c(58 \times 22)$ reconstruction was essentially pure Pt (*12a*). It is clear, therefore, that this structure is related to the "(1×5)" family of reconstructions observed on the (100) surfaces of Ir, Pt, and Au (*13*). It suggests that the surface of $CoPt_3(100)$ has a top layer of Pt atoms arranged in a "quasi-hexagonal" structure similar to the (111) surface of Pt. Such a surface structural model is shown in Fig. 2. The parameters of the primitive surface unit mesh are given in Table 1. The angle between the unit vectors is very nearly hexagonal (120.7°) and the orientation of the unit vectors is very nearly the same as that in the models developed for the pure Pt(100) reconstructed surface (*13*). The coincidences between the top layer and the substrate are arbitrarily shown in Fig. 2 to occur for the "on-top" sites. The bond lengths in this model, reported in Table 1, were calculated from the value of the bulk bond length of the substrate determined by X-ray diffraction, 2.72 Å, and are nearly identical to those of the pure Pt(100) reconstructed surface (*13*). Therefore, the outermost layer of this $CoPt_3(100)$ alloy surface appears to be constituted by a larger of pure Pt that adopts the *same structure* as in the pure Pt(100) surface, which is a quasi-hexagonal layer where the Pt–Pt bond lengths are ac-

TABLE 1

Parameters of Pt(100) and $CoPt_3(100)$ Surface Structures

Surface structure	Surface mesh dimensions (Å)	Angle between mesh unit vectors (degrees)
Pt(100)—1 × 1	2.77, 2.77	90
Pt(100)—$\begin{vmatrix}14 & 1\\ \bar{1} & 5\end{vmatrix}$	2.67, 2.67	119.8
$CoPt_3(100)$—1 × 1	2.72, 2.72	90
$CoPt_3(100)$ *c*(58 × 22)	2.66, 2.67	120.07

tually slightly shorter than in the (111) plane of pure Pt (*13*).

The (1 × 1) LEED pattern for the [111] oriented crystal and LEISS data indicating little or no (<2 at.% Co) Co in the top layer indicate "sandwich" enrichment of Pt in this surface as well. Angle-resolved XPS analysis of both the (111) and (100) surfaces also indicated that the second layer of atoms is enriched in Co relative to the bulk, e.g., 50–60 at.% versus the bulk 25 at.%. This "sandwich" type of enrichment was anticipated by some of the classical theories (*5*) of segregation phenomena, but has not been observed very frequently. A similar "sandwich" enrichment of Pt was observed by Gauthier *et al.* (*14*) for the [111] orientation of a $Pt_{78}Ni_{22}$ single crystal. In terms of alloy physical properties which constitute the parameters of segregation theories (*5*), Pt–Ni and Pt–Co are nearly identical. Recently, Treglia and Lagrand (*15*) proposed a mean-field theory incorporating lattice strain (the size effect), surface tension, and intermetallic bonding that predicts surface enrichment in Pt in the Pt–Ni system, but not to the extent of a 100% Pt surface (which was observed experimentally (*14*)).

The adsorption of CO at room temperature produced no ordered superstructures detectable by LEED. On the $CoPt_3(100)$ surface, prolonged exposure to CO caused the *c*(58 × 22) reconstruction to disappear, to be replaced by a simple (1 × 1) pattern. The lifting of the surface reconstruction by CO chemisorption is also a characteristic of the pure Pt(100) surface (*24*).

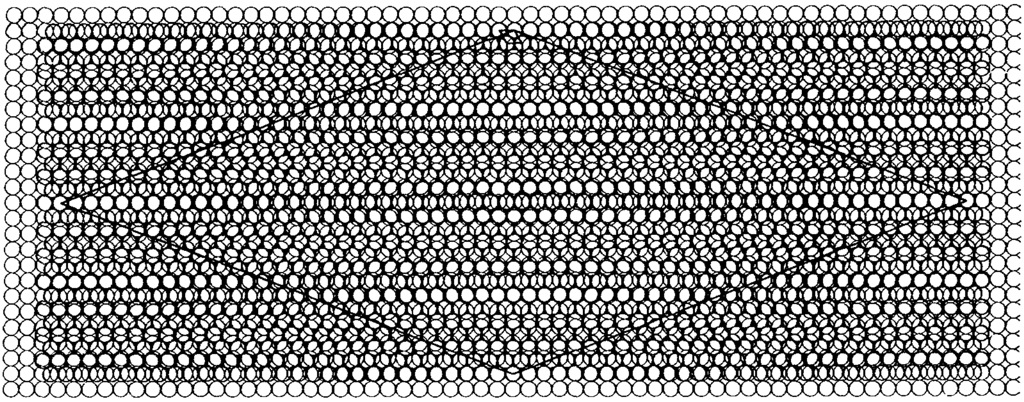

FIG. 2. Model of the *c*(58 × 22) "hexagonal" reconstructed surface of $CoPt_3(100)$. Reproduced from Ref. (*12b*).

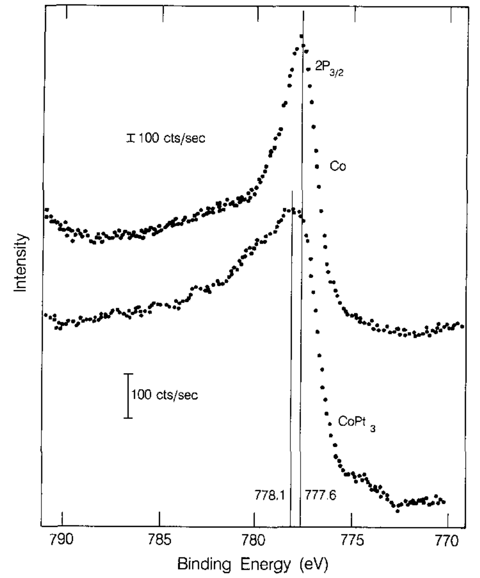

FIG. 3. Comparison of the Co $2P_{3/2}$ peak for a clean polycrystalline cobalt foil (upper curve) and for the clean, [100] oriented alloy surface. A similar result was obtained for the [111] oriented surface.

3.2 XPS

In Fig. 3 we show the Co $2P_{3/2}$ peak for the clean annealed (oxygen free) alloy surfaces compared with the same peak for a clean polycrystalline Co foil. There was clearly a shift of 0.5 eV toward higher binding energy for Co in $CoPt_3$ versus the pure metal. The Co $2P_{1/2}$ peak showed a similar shift. Platinum core level (4*f*) photoemission from the alloy was essentially unshifted with respect to the pure platinum surface. The +0.5-eV binding energy shift for Co in the $CoPt_3$ alloy is qualitatively similar to the +1.3-eV shift observed for Ti in the Pt_3Ti alloy (*16*), but not as large. In the case of Ti in Pt_3Ti, the shift for the alloy was as large as the shift for Ti in the cubic monoxide TiO, but here for Co in $CoPt_3$ the shift is about 0.8 eV less than the shift for the cubic monoxide CoO (*17*). It appears that the intermetallic bonding in $CoPt_3$ has some similarity to the bonding in Pt_3Ti (*26*), e.g., the solute atom in the alloy state has a lower electron density about its nucleus than does the same atom in the lattice of like solute atom, but the change from the state as the pure metal is not as dramatic for Co as that for Ti.

Another qualitative similarity in the intermetallic bonding can be seen in the (bulk) valence band structures, shown in Fig. 4. These should be compared with the spectra for Pt_3Ti given in Ref. (*7*). For both the $CoPt_3$ and Pt_3Ti alloys, there is an increase in the density of states at the bottom of the valence band (about 6 eV below the Fermi level), this increase being more pronounced in Pt_3Ti than in $CoPt_3$. If we combine both the core level shifts with the changes in the valence band density of states, an elementary interpretation is that in forming the intermetallic bonds in these alloys, there is a rehybridization of *d*-orbitals of the solute atom that are nonbinding (atomic-like) in the pure solute metal to form bonding orbitals in the alloy, which results in a shift in electron density from about the solute atom to the interatomic region.

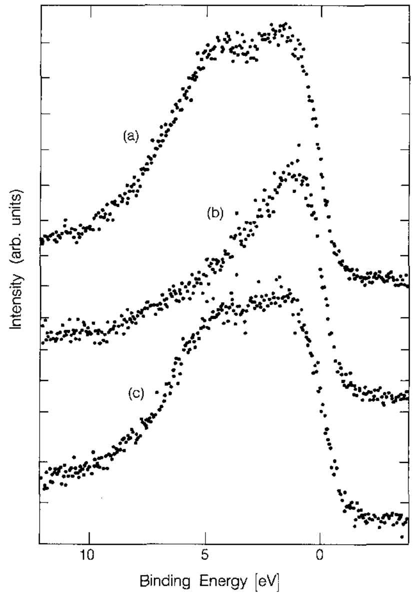

FIG. 4. Comparison of the valence band structure for clean (100) platinum (top curve), clean polycrystalline Co (middle curve), and the clean [100] oriented $CoPt_3$ surface (bottom curve).

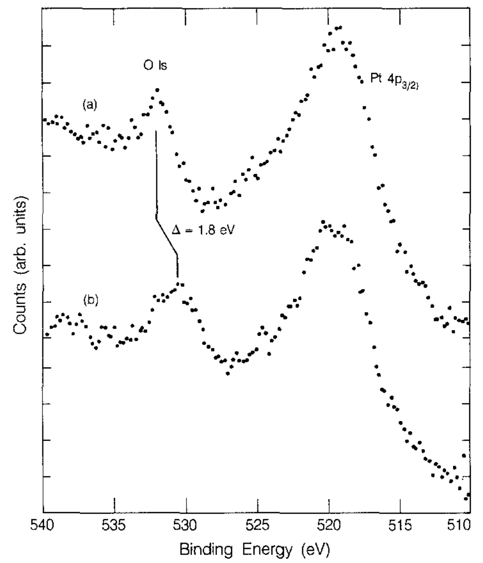

FIG. 5. Comparison of O 1*s* peak for (a) carbon monoxide and (b) oxygen chemisorbed to saturation at 298 K on [111] oriented $CoPt_3$.

The adsorption of carbon monoxide on the clean alloy surface could be detected in XPS by the appearance of the oxygen and carbon 1*s* peaks. The O 1*s* peak resulting from adsorbed CO was shifted by 1.8 eV toward higher binding energy with respect to the oxygen peak for oxygen chemisorbed on the surface (Fig. 5). This is the same shift we observed for the chemisorption of CO on pure Pt surfaces. The asymmetric shape of the O1*s* peak, with the shoulder on the high energy side, is identical to the spectrum reported by Norton *et al.* (*18*) for CO on Pt(111) and quite different from the doublet spectrum we reported previously (*7*) for $Pt_3Ti(111)$. We attributed the doublet structure as arising from the distinctly different bonding geometries predicted for CO at Pt and Ti sites (*2*) in the $Pt_3Ti(111)$ surface. Flashing the crystal to >900°K completely removed all oxygen *and* carbon detectable by XPS, showing that no detectable decomposition of CO took place during desorption. This result indicates a substantial difference in the interaction of CO with the $CoPt_3$ alloy in comparison to our results with the Pt_3Ti alloy, where ca. 25% of CO molecules adsorbed were dissociated even at low temperature (>330°K) (*7*). However, the absence of dissociation is similar to the observation by Paul *et al.* (*11*) on their Pt-enriched $Pt_3Ti(111)$ surface.

3.3 TDS

In Fig. 6 we show the thermal desorption spectra recorded from the [111] and [100] oriented alloy surfaces after adsorption to saturation with CO. The CO TDS peak for a polycrystalline $CoPt_3$ surface was similar to that of the [111] surface. The shape of the CO TDS spectrum from the $CoPt_3(111)$ surface is qualitatively similar to the spectrum observed on the Pt(111) surface by various authors (*19–24*) although it occurs at a significantly lower temperature. Also, the maximum in the broad spectrum for the $CoPt_3(100)$ surface occurred at a considerably lower temperature than the main peak from pure Pt(100) (*22, 23*). For exposure to CO to lower than saturation coverages, we found the same behavior that has been re-

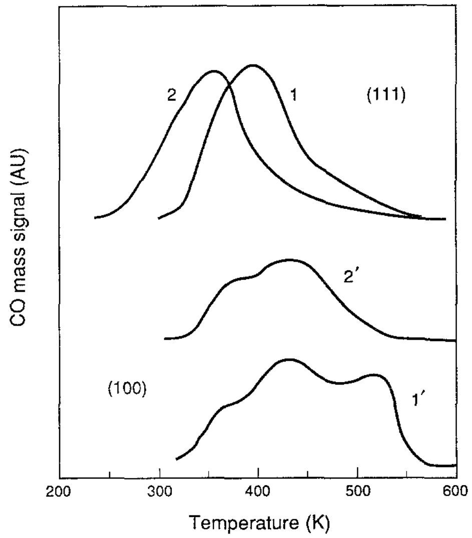

FIG. 6. CO thermal desorption after 10 Langmuirs exposure at 300°K from the [100] surfaces of pure Pt (1′) and $CoPt_3$ (2′); at 250°K from the [111] surfaces of pure Pt (1) and $CoPt_3$ (2). Heating rate: ca. 15°K/s in all cases (see text).

ported for pure platinum surfaces (*19–23*), i.e., a shift in the maximum of the CO TDS peak toward higher temperatures for lower coverages. On both the [111] and [100] oriented surfaces of $CoPt_3$, saturation coverage by CO was somewhat lower than that found on the pure Pt surface of the same orientation, e.g., 60–70%.

The observation of purely molecular CO desorption from the $CoPt_3$ surfaces is not surprising, considering that the surface composition of these surfaces is essentially pure Pt, and it is well known that CO does not dissociate on clean Pt surfaces. For the CO desorbing molecularly from the Pt sites, the TDS spectra for the Pt_3Ti(111) surface (*7, 11*) were very similar to the result here for $CoPt_3$(111), with a peak temperature of 360–370°K. Using the Redhead (*25*) analysis for TDS, the 50°K difference between the peak temperatures from the two alloy (111) surfaces and the Pt(111) surface means an activation energy for desorption that is ca. 15% lower on the alloy surfaces. For the $CoPt_3$(100) surface, the difference is even larger, corresponding to an activation energy that is 22% lower than for the Pt(111) surface.

It is well known that CO is a useful molecule for probing electronic effects in alloy surfaces due to the sensitivity of the CO–metal bond to the *d*-orbital configuration of the metal. However, it is also well known that one must consider structural effects (so-called "ensemble" effects) in addition to electronic effects when interpreting the effect on adsorbate bonding of dispersing a solute metal atom in the surface of another metal. In our analysis of CO bonding to Pt_3Ti surfaces (*2*), we used a quantum chemical treatment to examine both ensemble effects, e.g., the elimination of some Pt–Pt bridge sites and Pt fourfold hollows, as well as the effect of intermetallic bonding on the kind and number of orbitals available for bonding CO to Pt sites. The ASED–MO calculations (*2*) showed that even for CO bound to *a*-top Pt sites (i.e., no ensemble effect), the use of Pt *d*-electrons to form intermetallic bonds with Ti reduces the back-bonding contribution to the total CO–Pt bond energy. In the case of the $CoPt_3$ surfaces, the clean annealed surfaces are essentially pure Pt, so there can be no ensemble effect due to Co dispersed in the topmost layer. There is, nonetheless, a significant difference (15–20% lower bond energy) in CO bonding to this pure Pt surface layer, presumably due to intermetallic bonding of Pt surface atoms with the Co atoms in the second layer. We have presented core level and valence band spectroscopy which indicate that there are qualitative similarities in the *bulk* electronic properties of $CoPt_3$ and Pt_3Ti, and we now suggest that the general features of the ASED–MO bond model for Pt_3Ti also apply to $CoPt_3$. It is surprising, however, that the effects of intermetallic bonding are so significant, given that the Co–Pt bond energy is so much lower than the Ti–Pt bond energy.

The effect of intermetallic bonding on CO bond energy that we found here for a pure Pt top-layer produced by surface segregation from a Co–Pt alloy bulk crystal bears some similarity to recent studies of CO chemisorption on certain pure metal monolayers on dissimilar metal substrates (*27*). Particularly relevant is the study by Strongin and co-workers (*28*) of a Pt monolayer on Ta(110). Like Pt–Ti, Pt–Ta alloys have very exothermic heats of formation (*9*) and exhibit strong intermetallic bonding. The CO–Pt bond energy was reported to be much weaker when chemisorbed on the Pt monolayer on Ta(110) than on the Pt multilayer, an effect attributed directly (by use of photoemission spectroscopy of the bonding orbitals) to a reduction of back-bonding to the CO $2\pi^*$ orbitals by the *d*-electrons of the metal monolayer. A qualitatively similar reduction of CO bond energy was also found for Ni when Ni monolayers were deposited on W(110) and (100) (*29*). Thus, one could view the results reported here for the CO–Pt alloy as one of the first examples where a pure metal monolayer produced by surface segregation in a binary alloy exhibited chemisorptive properties characteristic of a number of the synthetic metal monolayer systems. Therefore, it should be possible to use the property of surface segregation in binary alloys to reduce to catalytic practice the interesting electronic effects of intermetallic bonding observed in many of the synthetic metal monolayer systems (*27*).

ACKNOWLEDGMENT

This work was supported in part by the Assistant Secretary for Fossil Energy, Office of Coal Utilization, Advanced Conversion and Gasification, Advanced Energy Conversion Systems Division of the U.S. Department of Energy under Contract DE-AC03-76SF00098, and in part by the Consiglio Nationale delle Recerche, Italy.

REFERENCES

1. Brewer, L. *in* "Phase Stability in Metals and Alloys" (P. Rudman and R. I. Jaffee, Eds.), p. 39. McGraw–Hill, New York, 1967.

2. Mehandru, S. P., Anderson, A. B., and Ross, P. N., *J. Catal.* **100,** 210 (1986).

3. Horsley, J. A., *J. Amer. Chem. Soc.* **101,** 2870 (1979).

4. Kelley, M. J., and Ponec, V., *Prog. Surf. Sci.* **11,** 139 (1981).

5. Sachtler, W. M. H., and Van Santen, R. A., *Appl. Surf. Sci.* **11,** 139 (1981); *in* "Advances in Catalysis" (D. D. Eley, H. Pines, and P. B. Weisz, Eds.), Vol. 26, p. 69. Academic Press, San Diego, 1977.

6. Bardi, U., Ross, P. N., and Somorjai, G. A., *J. Vac. Sci. Technol.* **A2,** 1467 (1984).

7. Bardi, U., Dahlgran, D., and Ross, P. N., *J. Catal.* **100,** 196 (1986).

8. Bardi, U., and Ross, P. N., *Surf. Sci.* **146,** L555 (1984).

9. Hultgren, R., Orr, R. L., Anderson, P. P., and Kelley, K. K., Eds., "Selected values of Thermodynamic Properties of Metals and Alloys," p. 647. New York and London 1962.

10. (*a*) Moffatt, W., "The Handbook of Binery Phase Diagrams," Genium, Schenectady, NY, 1984. (*b*) Gebhardt, E., and Koster, W., *Z. Metallkd.* **32,** 253 (1940).

11. Paul, J., Cameron, S., Dwyer, D., and Hoffman, F., *Surf. Sci.* **177,** 121 (1986).

12. (*a*) Bardi, U., Atrei, A., Ross, P., Zanazzi, E., and Rovida, G., *Surf. Sci.* **211/212,** 441 (1989). (*b*) Bardi, U., Atrei, A., Ross, P., Zanazzi, E., and Rovida, G., *Vacuum,* in press.

13. Van Hove, M. A., Koestner, R. J., Stair, P . C., Biberian, J. P., Kesmodel, L. L., Bartos, I., and Somorjai, G. A., *Surf. Sci.* **103,** 189 (1981).

14. Gauthier, Y., Joly, Y., Baudoing, R., and Rundgren, J., *Phys. Rev. B* **31** 6216 (1985).

15. Treglia, G., and Legrand, B., *Phys. Rev. B* **35** 4338 (1987).

16. Beard, B., and Ross, P. N., *J. Phys. Chem.* **90,** 6811 (1986).

17. Bardi, U., Beard, B., and Ross, P. M., *J. Vac. Sci. Technol. A* **6,** 665 (1988).

18. Norton, P., Goodale, J., and Selkirk, E., *Surf. Sci.* **83,** 189 (1979).

19. Ertl, G., Neumann, M., and Streit, K. M., *Surf. Sci.* **64,** 393 (1977).

20. McCabe, R. W., and Schmidt, L. D., *Surf. Sci.* **66,** 101 (1977).

21. Collins, D. N., and Spicer, W. E., *Surf. Sci.* **69,** 85 (1977).

22. Barteau, M. A., Ko, E. I., and Madix, R. J., *Surf. Sci.* **102,** 99 (1981).

23. Crossley, A., and King, D. A., *Surf. Sci.* **95,** 131 (1980).

24. Thiel, P., Behm, R., Norton, P., and Ertl, G., *J. Chem. Phys.* **78,** 7448 (1983).

25. Redhead, P., *Vacuum* **12,** 203 (1962).

26. A complete discussion of the interpretation of core-level shifts in these intermetallic systems is beyond the scope of this paper. A more detailed discussion of our interpretation may be found in G. Derry and P. Ross, *Sol. State Comm.* **52,** 151 (1984). An excellent and more complete discussion of binding energy shifts in intermetallic systems was presented by G. Wertheim, D. Buchanan, and J. Wernick, *Phys. Rev. B* **40** 5319 (1989).

27. Berlowitz, P., Peden, D., and Goodman, D., *in* "Physical and Chemical Properties of Thin Metal Overlayers and Alloy Surfaces" (D. Zehner and D. Goodman, Eds.), Vol. 83, p. 161. The Materials Research Society, Pittsburgh, PA, 1987; and other papers in this volume.

28. Ruckman, M., Strongin, M., and Pan, X., *J. Vac. Sci. Technol. A* **5,** 805 (1987).

29. Berlowitz, P., and Goodman, D., *Surf. Sci.* **187,** 463 (1987).